Anisotropic Thermopower and Planar Nernst Effect in $Ga_{1-x}Mn_xAs$ Ferromagnetic Semiconductors

Yong Pu,[1] E. Johnston-Halperin,[2] D. D. Awschalom,[2] and Jing Shi[1]
[1]*Department of Physics, University of California, Riverside, California 92521, USA*
[2]*Department of Physics, University of California, Santa Barbara, California 93106, USA*
(Received 5 May 2006; published 20 July 2006)

We present the first experimental study of the thermopower in Mn-doped GaAs ferromagnetic semiconductors. Large magnetothermopower effects in both longitudinal and transverse directions have been observed below the ferromagnetic transition temperature. Unlike magnetoresistance, neither the transverse thermopower (planar Nernst effect) nor the longitudinal thermopower explicitly depend on the strength of the in-plane magnetic field, but rather are intimately related to each other through the magnetization. These newly discovered effects can be satisfactorily explained by an extension of anisotropic magnetotransport model and place important constraints on potential microscopic descriptions of the scattering mechanisms in these materials.

DOI: 10.1103/PhysRevLett.97.036601 PACS numbers: 72.20.Pa, 73.50.Lw, 75.50.Pp

Mn-doped III-V semiconductors, a class of prototypical materials that can potentially be used in spintronics applications, have been extensively studied. In the course of that study, a host of interesting transport phenomena, such as anisotropic magnetoresistance [1–3], tunneling magnetoresistance [4–6], giant planar Hall effect [7], and the Kondo effect [8], have been reported recently in these materials.

Typically, previous transport studies have been focused on electrical resistivity. However, another important transport coefficient, thermoelectric power (thermopower), is uniquely capable of probing carrier properties (electron or hole) as well as scattering mechanisms in solids and has so far not been explored in this system. In this work, we present the first systematic experimental study of thermopower and magnetothermopower in $Ga_{1-x}Mn_xAs$ using three different Mn concentrations ($x = 0.039$, 0.049, and 0.059). First, we found that the thermopower is positive in all three samples, which is a generic property of hole systems. We also found that the magnitude of the thermopower depends on the relative direction of the magnetization with respect to the temperature gradient. Finally, we are reporting here a new phenomenon, that there exists a giant transverse thermal electromotive force (EMF), or Nernst voltage, that is sensitive to the in-plane magnetization. We will show that both the longitudinal magnetothermopower $S_{xx}(H)$ and the transverse magnetothermopower [planar Nernst effect (PNE)] $S_{xy}(H)$ share a common origin, which is related to the anisotropic scattering rate in the ferromagnetic phase of the dilute magnetic semiconductors.

All (Ga,Mn)As samples were grown by molecular beam epitaxy (MBE) in a Varian-EPI GenII MBE chamber. The samples were grown at a substrate temperature of 250 °C with dynamic temperature control provided by optical band-edge thermometry and under an overpressure of cracked As_4. Samples were not annealed after growth [9]. The films were then patterned into Hall bars with a width of 0.1–1 mm using standard photolithography. Most Hall bars were defined along the $[\bar{1}10]$ direction. For a comparison study, an additional Hall bar was defined along the [110] direction for one sample.

During our measurements, the temperature rise ΔT_x between the two voltage leads (with a separation of ~10 mm) was typically set at ~0.1–0.5 K. ΔT_x was measured by a fine type-E differential thermocouple attached close to the voltage leads. Meanwhile, we also measured the heat-on and -off sample resistances, R_{on} and R_{off}, using the *same* voltage leads. These values were then used to convert the sample resistance change, $\Delta R = R_{off} - R_{on}$, to ΔT_x using a resistance vs temperature calibration curve measured separately for each sample. We found using the sample resistance as our thermometry to be more accurate than the thermocouple method because both ΔT_x and thermal EMF ΔV_x are generated by the exactly same segment of the sample [10].

To measure thermopower, we adopted a step-heating method. Heater power steps up then down in several discrete levels to generate a series of ΔT_x. At the same time, the corresponding longitudinal (transverse) thermal EMF signal ΔV_x (ΔV_y) is recorded as a function of ΔT_x [lower inset of Fig. 1(a)]. By a linear fit [11] we obtained the slope, which is the longitudinal or the transverse thermopower. To measure magnetothermopower, we swept an in-plane magnetic field H using an electromagnet (up to 2.5 kOe) while recording ΔV_x or ΔV_y. Since we did not find any appreciable change in heater power as the field was swept up to 2.5 kOe, the field dependence of ΔV_x or ΔV_y was directly converted to magnetothermopower for a fixed ΔT_x.

Figure 1(a) shows the angular dependence of S_{xx} as a function of H for $Ga_{0.961}Mn_{0.039}As$ measured at $T = 6$ K. The temperature gradient ∇T was directed along $[\bar{1}10]$, and the orientation of the in-plane field $\boldsymbol{H}$ was varied from being parallel ($\Phi_H = 0$) to perpendicular ($\Phi_H = 90°$) to ∇T in the plane of the sample. For a fixed angle Φ_H, as $\boldsymbol{H}$

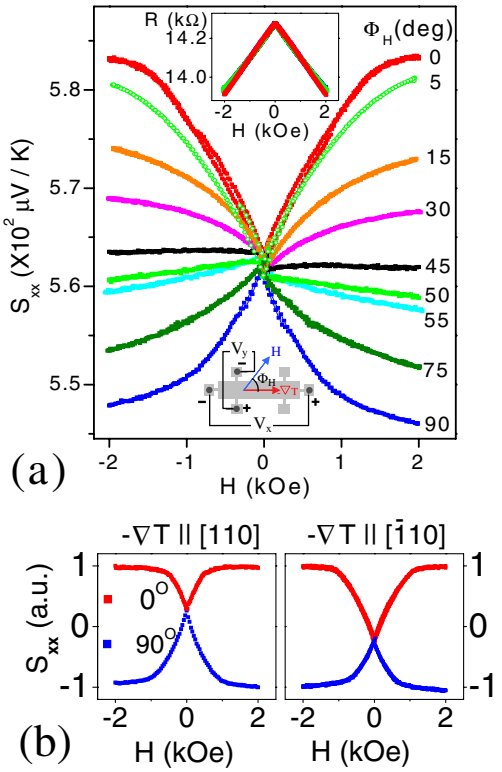

FIG. 1 (color online). (a) Angular dependence of longitudinal magnetothermopower S_{xx} at 6 K; the sample is $Ga_{1-x}Mn_xAs$ ($x = 0.039$) and heat flow is applied in the $[\bar{1}10]$ direction. Top inset shows the angular dependence of magnetoresistance of the sample, and the bottom inset is a sketch of the relative orientation of heat flow $-\nabla T$ and external field $\boldsymbol{H}$. (b) S_{xx} vs H when the applied heat flow is in the $[110]$ and $[\bar{1}10]$ directions at 15 K.

increases, S_{xx} either increases or decreases depending on Φ_H, and saturates at $H \sim 2$ kOe. At saturation, $S_{xx}(\Phi_H = 0°)$ is greater than $S_{xx}(\Phi_H = 90°)$. Since the sample magnetization $\boldsymbol{M}$ should be fully aligned with $\boldsymbol{H}$ at saturation, which is also corroborated by separate magnetization measurements [12], we have $S_{||} > S_{\perp}$. Here $S_{||}$ ($S_{\perp}$) is the saturation longitudinal thermopower when $\boldsymbol{M}$ is parallel (perpendicular) to ∇T. At 6 K, $\Delta S/S = (S_{||} - S_{\perp})/S_0 \sim 6\%$, and it decreases as the temperature is raised. This anisotropic thermopower effect resembles the usual anisotropic magnetoresistance (AMR) phenomenon in ferromagnetic metals, which is accounted for by the spin-orbit interaction [13] that leads to different scattering rates or resistivities between current parallel and perpendicular to $\boldsymbol{M}$ (typically $\rho_{||} > \rho_{\perp}$). In ferromagnetic semiconductors, similar AMR exists; however, it is found that $\rho_{||} < \rho_{\perp}$ [1,2,7], opposite to that in metals. Another unique characteristic of ferromagnetic semiconductors is that the resistivity strongly depends on H even above the saturation of $\boldsymbol{M}$ [inset of Fig. 1(a)] [2]. In contrast, S_{xx} shows clear saturation, which is more evident at high temperatures [Fig. 1(b)] when the saturation field becomes smaller.

The strong angular dependence and saturation demonstrates that thermopower senses the direction and magnitude, respectively, of $\boldsymbol{M}$ (rather than $\boldsymbol{H}$). For example, at $\Phi_H = 45°$, S_{xx} does not strongly depend on $\boldsymbol{H}$ except at very small fields. This special direction is close to an easy axis of the sample, in which $\boldsymbol{M}$ does not rotate but rather switches at critical values in a small field region. Note that in Fig. 1(a) there is an asymmetry in S_{xx} between the positive and negative $\boldsymbol{H}$ directions. This asymmetric background behaves like a step function, which is clearly seen at $\Phi_H \sim 45°$, where very little magnetization rotation-related background is present. We also found that the step height is proportional to $\cos(\Phi_H)$ or the y component of $\boldsymbol{M}$.

One possible origin of the asymmetry is the unidirectional anisotropy caused by an exchange bias mechanism. To test this possibility, we cooled the sample from high temperatures ($\gg T_c$) in nonzero $\boldsymbol{H}$ with different Φ_H, but the asymmetry was not affected. This argues against the exchange bias scenario. Another viable alternative is that, due to a small unavoidable temperature gradient along the sample normal $(\nabla T)_z$, the anomalous Nernst effect, the counterpart of the anomalous Hall effect [14], could give rise to an additional voltage ΔV_x along the Hall bar if there is a nonzero in-plane magnetization component along the y axis (M_y). The anomalous Nernst signal should be proportional to M_y, or $\cos(\Phi_H)$. This scenario is apparently consistent with the experimental fact that the step height of the observed asymmetric background in S_{xx} is proportional to M_y. Further investigation of this effect is currently underway.

To determine the role of crystallographic orientation in anisotropic thermopower, we also patterned a Hall bar along $[110]$ and measured S_{xx} with the heat flow along $[110]$. In Fig. 1(b), S_{xx} with $-\nabla T$ along both $[110]$ and $[\bar{1}10]$ is displayed side by side. It is evident that S_{xx} approaches the same final value $S_{||}(S_{\perp})$ as long as $\boldsymbol{M}$ is oriented parallel (perpendicular) to the direction of hear flow no matter whether $\boldsymbol{M}$ lies in $[110]$ or $[\bar{1}10]$, or which path S_{xx} actually takes to the final saturation value. This is distinct from the tunneling anisotropic magnetoresistance effect found in similar materials, in which the magnitude of the effect depends on which crystallographic direction (e.g., $[100]$ or $[010]$) $\boldsymbol{M}$ lies along [15].

We have also found a magnetothermopower effect in the transverse direction, as shown in Fig. 2(a). Both effects exist in all three samples, only differing in magnitude. At $H = 0$ when $\boldsymbol{M}$ lies along one of the easy axis directions (e.g., close to $[100]$), there is a large transverse signal $S_{xy} \sim 15\ \mu$V/K. S_{xy} changes in a nonmonotonic way as the in-plane magnetic field is continuously swept. This nonzero off-diagonal thermopower component is similar to but much greater than the conventional Nernst effect ($\sim$10 nV/K per Tesla of magnetic field [16–18]). Here $\boldsymbol{H}$ is applied in the plane of the Hall bar; therefore, we call the effect here the PNE.

Analogous to the planar Hall effect [7] found in similar systems, the PNE shows two distinct switchings in each

field sweep. These switching fields in PNE curves correspond well to those appearing in planar Hall measured in the same sample [bottom panel of Fig. 2(a)]. As discussed by Tang *et al.* [7], in the presence of both uniaxial and fourfold anisotropies, the easy directions are determined by the relative strength of the two anisotropies. Let us assume that the uniaxial anisotropy is relatively weak. If $\boldsymbol{H}$ is swept from "+" to "−" at $\Phi_H = -30°$ as shown in Fig. 2(b), $\boldsymbol{M}$ makes the first transition from the initial direction $-\Phi_0$ [state I in Fig. 2(b)] to an intermediate direction, Φ_0 (state II), and then the second transition occurs from Φ_0 (state II) to $-\Phi_0 + 180°$ (state III), which completes the full reversal of $\boldsymbol{M}$. As $\boldsymbol{H}$ is reversed, a different route is followed, namely, III → IV → I, and hysteresis occurs, as shown in the figure. According to the following two equations, which can be obtained by substituting ρ_x by S_{xx}, ρ_y by S_{xy}, $\rho_{||}$ by $S_{||}$, and $\rho_\perp$ by $S_\perp$ in the AMR equations [19], both transitions ($-\Phi_0 \rightarrow \Phi_0$ and $\Phi_0 \rightarrow -\Phi_0 + 180°$) will produce discontinuous jumps in S_{xy} at two fields, but neither transition will be registered in S_{xx}. Here Φ is the angle between $\boldsymbol{M}$ and $-\nabla T$.

$$S_{xx} = \tfrac{1}{2}[(S_{||} + S_\perp) + (S_{||} - S_\perp)\cos 2\Phi], \quad (1)$$

$$S_{xy} = \tfrac{1}{2}(S_{||} - S_\perp)\sin 2\Phi. \quad (2)$$

From the direction of jumps in S_{xy}, one immediately obtains $\Delta S = S_{||} - S_\perp > 0$, which agrees with the earlier conclusions from S_{xx} measurements. As the field direction is varied, we also measured the angular dependence of PNE for a series of Φ_H [Fig. 2(c)]. As Φ_H changes from positive to negative, the jumps in S_{xy} are inverted, as expected from Eq. (2). Furthermore, the switching field also changes as a function of Φ_H, and this is fully consistent with the two-anisotropy model as discussed in the planar Hall case [7].

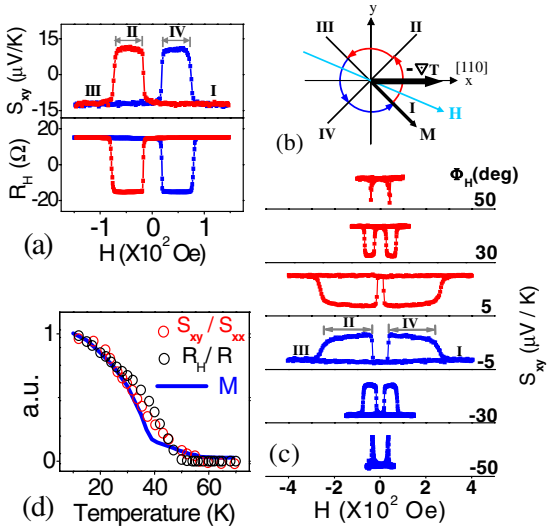

FIG. 2 (color online). (a) Planar Nernst effect (PNE) and planar Hall effect at 6 K $\Phi_H = -30°$ for $Ga_{1-x}Mn_xAs$ ($x = 0.039$). (b) Sketch of the relative orientation of $-\nabla T$, $\boldsymbol{M}$ and $\boldsymbol{H}$. Four directions marked as I, II, III, and IV are easy directions of $\boldsymbol{M}$. (c) Angular dependence of PNE. (d) Comparison of S_{xy}/S_{xx} and R_H/R, and sample magnetization M measured by SQUID.

The size of the PNE jumps is a measure of the anisotropy in transport which is ultimately related to the spin-orbit interaction strength of the material. We plot the jump in PNE normalized by the longitudinal thermopower S_{xx} as a function of temperature [Fig. 2(d)]. This ratio decreases steadily as the temperature increases, and eventually approaches zero as $\boldsymbol{M}$ vanishes at T_c. This general trend agrees with that of $\boldsymbol{M}$ and the planar Hall resistance.

The two anisotropic thermopower equations should link S_{xx} and S_{xy} at any arbitrary field through the angle Φ. Here we assume that the direction of $\boldsymbol{M}$ of the entire sample can be represented by a *single* Φ; i.e., the whole sample behaves as a single-domain object and rotates coherently as $\boldsymbol{H}$ varies. The single-domain assumption is supported by the S_{xx} vs $\boldsymbol{H}$ curve for $\Phi_H = 45°$, where no distribution in easy axis is seen as evidenced by the flat background. Next, to show the correlation between S_{xx} and S_{xy}, we first compute the angle Φ_x from measured S_{xx} at a given field, shown in Fig. 3(a) (left panel); then we compute the corresponding $\sin(2\Phi_x)$ as a function of $\boldsymbol{H}$. Meanwhile, we also compute $\sin(2\Phi_y)$ from the experimentally measured S_{xy} [Fig. 3(a), right panel]. If the single-domain model holds, i.e., the sample magnetization can be represented by a single variable Φ, these two curves should agree with each other. As mentioned earlier, magnetization switching does appear in S_{xy} but not in S_{xx}; therefore, $\sin(2\Phi_y)$ computed from S_{xy} should fall on either $\sin(2\Phi_x)$ or its inverse $-\sin(2\Phi_x)$ computed from S_{xx}. The excellent agreement between two measurements as seen in Fig. 3(b) shows that S_{xx} and S_{xy} obey the equations very well.

This is in stark contrast with the relationship between ρ_{xx} and ρ_{xy} in the case of electrical transport, where only the latter obeys the second equation. ρ_{xx} depends on both $\boldsymbol{H}$ and $\boldsymbol{M}$, whereas ρ_{xy} depends strongly on $\boldsymbol{M}$ but only very weakly on $\boldsymbol{H}$. This implies that $\rho_{||}$ and $\rho_\perp$ each depends on $\boldsymbol{H}$ strongly, but that they differ by a factor very close to 1 because the former contains $\rho_{||} + \rho_\perp$ but the latter contains $\rho_{||} - \rho_\perp$ [inset of Fig. 1(a)]. The strong field dependence of ρ_{xx} was previously attributed to the suppression of weak localization at low temperatures and suppression of spin disorder scattering at high temperatures [2,20,21]. However, neither longitudinal nor transverse thermopower explicitly depends on $\boldsymbol{H}$ at low temperatures. Thermopower $S_{||}$ ($S_\perp$) and resistivity $\rho_{||}$ ($\rho_\perp$) are related by the Mott formula [22] $S = -\frac{\pi^2 k_B^2 T}{3e}\left(\frac{\partial \ln\rho}{\partial E}\right)_{E_F}$. The absence of $\boldsymbol{H}$ dependence in S_{xx} or S_{xy} suggests that $\boldsymbol{H}$ dependence must be factored out from the energy dependence in $\rho_{||}$ and $\rho_\perp$, so that it disappears in S_{xx} and S_{xy} after the derivative is taken of $\ln(\rho)$. For example, if the scattering has both $\boldsymbol{H}$-dependent and $\boldsymbol{H}$-independent processes, then, similar to Matthiessen's rule, the total scat-

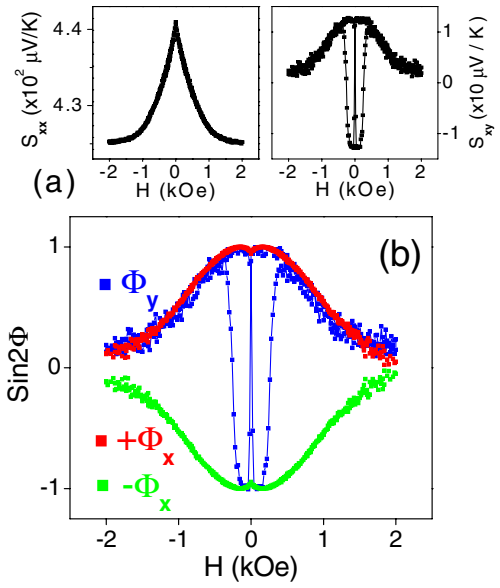

FIG. 3 (color online). (a) Field dependence of S_{xx} and S_{xy} measured at $T = 12$ K, $\Phi_H = 90°$ for sample $Ga_{1-x}Mn_xAs$ ($x = 0.049$). Heat flow is applied along the [110] direction. (b) Field dependence of the magnetization angle Φ—the angle between $\boldsymbol{M}$ and the heat flow $-\nabla T$, Φ_x, and Φ_y are calculated from S_{xx} and S_{xy} data as described in the text.

tering rate would be the sum of the two; therefore, the $\boldsymbol{H}$-dependent factor does not always trivially factor out.

Finally, let us assume the single-domain model and use the thermopower as a tool to study the magnetic anisotropy of the ferromagnetic semiconductors. Assume the following anisotropy energy: $E_K = K_u \sin^2\Phi + (K_c/4)\cos^2 2\Phi$, the first term being the uniaxial anisotropy and the second the cubic anisotropy with anisotropic constants K_u and K_c,

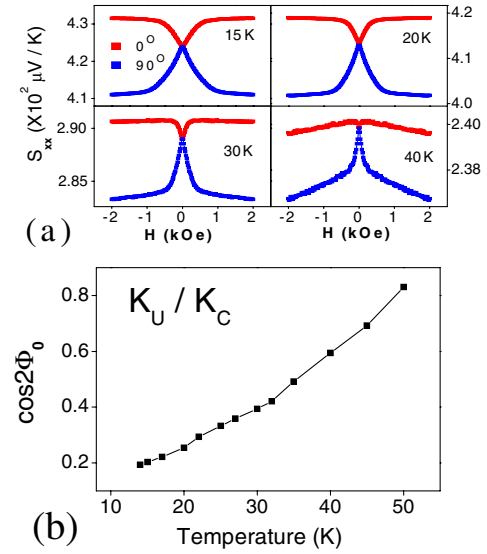

FIG. 4 (color online). (a) Temperature dependence of S_{xx} for sample $Ga_{1-x}Mn_xAs$ ($x = 0.049$) with the heat flow applied in the [110] direction. (b) Temperature dependence of the ratio of uniaxial to cubic anisotropy constants.

respectively. At $\boldsymbol{H} = 0$, the easy axes are determined by $\cos(2\Phi) = K_u/K_c$. The extracted K_u/K_c from Fig. 4(a) is then plotted in Fig. 4(b). At low temperatures, the anisotropy is clearly dominated by the cubic crystalline anisotropy. If the curve is extrapolated to 4 K, the ratio agrees well with that obtained from the planar Hall measurements at 4 K [7]. As the temperature approaches T_c, the cubic anisotropy clearly gives away to the uniaxial anisotropy. This is consistent with other findings in similar materials [23].

In summary, anisotropic thermopower is shown to be a very important transport property of ferromagnetic semiconductors. Both longitudinal and transverse magnetothermopower effects are intimately related through the sample magnetization. In conjunction with magnetoresistivity, thermopower may provide additional important microscopic scattering information in the materials due to its sensitivity to the energy derivative of $\ln(\rho)$.

J. S. would like to acknowledge Professor X. R. Wang for many valuable discussions. Y. P. and J. S. were supported by DOE and CNID; E. J.-H. and D. D. A. were supported by NSF and AFOSR.

[1] T. Jungwirth *et al.*, Appl. Phys. Lett. **83**, 320 (2003).
[2] F. Matsukura *et al.*, Physica (Amsterdam) **21E**, 1032 (2004).
[3] K. Y. Wang *et al.*, Phys. Rev. B **72**, 085201 (2005).
[4] M. Tanaka and Y. Higo, Phys. Rev. Lett. **87**, 026602 (2001).
[5] D. Chiba, F. Matsukura, and H. Ohno, Physica (Amsterdam) **21E**, 966 (2004).
[6] C. Rüster *et al.*, Phys. Rev. Lett. **94**, 027203 (2005).
[7] H. X. Tang *et al.*, Phys. Rev. Lett. **90**, 107201 (2003).
[8] H. T. He *et al.*, Appl. Phys. Lett. **87**, 162506 (2005).
[9] R. K. Kawakami *et al.*, Appl. Phys. Lett. **77**, 2379 (2000).
[10] Y. Pu *et al.*, in *Proceedings of the Third Student-Organizing International Mini-Conference on Information Electronics System (SOIM-COE05), Sendai, Japan, 2005* (Tohoku University, Sendai, 2005), pp. 27–30.
[11] Over the range of 0.1–0.5 K in ΔT_x, we found excellent linearity between thermal EMF ΔV_x or ΔV_y and ΔT_x.
[12] The magnitude of M stays constant when H reaches the saturation field in M vs H hysteresis loops.
[13] S. Chikazumi, *Physics of Ferromagnetism* (Clarendon Press, Oxford, 1997), p. 590.
[14] L. Berger and Bergmann, in *The Hall Effect and Its Applications*, edited by C. L. Chien and C. R. Westgate (Plenum, New York, 1980), p. 55.
[15] C. Gould *et al.*, Phys. Rev. Lett. **93**, 117203 (2004).
[16] Z. A. Xu *et al.*, Nature (London) **406**, 486 (2000).
[17] J. A. Clayhold *et al.*, Phys. Rev. B **50**, 4252 (1994).
[18] M. Zeh *et al.*, Phys. Rev. Lett. **64**, 3195 (1990).
[19] J. P. Pan, *Solid State Physics*, edited by F. Seitz and D. Turnbull (Academic, New York, 1957), Vol. 5, pp. 1–96.
[20] T. Omiya *et al.*, Physica (Amsterdam) **7E**, 976 (2000).
[21] K. W. Edmonds *et al.*, J. Appl. Phys. **93**, 6787 (2003).
[22] N. F. Mott and H. Jones, *The Theory of the Properties of Metals and Alloys* (Dover, New York, 1958), p. 308.
[23] K. Y. Wang *et al.*, Phys. Rev. Lett. **95**, 217204 (2005).